2D modelling of a dry joint masonry wall retaining a pulverulent backfill

Anne-Sophie Colas [a], Jean-Claude Morel [a,*], Denis Garnier [b]

[a] *Université de Lyon, Département Génie Civil et Bâtiment (CNRS, URA 1652), École Nationale des Travaux Publics de lÉtat, rue M. Audin, 69518 Vaulx-en-Velin cedex, FRANCE.*

[b] *Université Paris-Est, UR Navier, École Nationale des Ponts et Chaussées, 6-8 avenue B. Pascal, 77455 Marne-la-Vallée cedex 2 , FRANCE.*

Abstract

This study focuses on an analysis of dry joint retaining structures based on yield design theory: the stability of the masonry is assessed using rigid block and shear failure mechanisms in the wall and its backfill. An application of this simulation on 2D scale-down brick and wood models is then addressed, showing close agreement between theoretical predictions and experimental results. Further development on this work, including application of this theory on dry-stone retaining walls, are discussed as a conclusion.

Key words: Dry joint stone masonry, retaining walls, yield design, 2D scale-down experiments

1 Introduction

Masonry structures have received great attention over the past few decades, fairly due to the growing interest in the maintenance and repair of heritage and historical architecture. Part of these masonry constructions were built dry or have experienced a loss of mortar due to aging and can now be considered as dry joint structures.

This study focuses on dry joint masonry retaining constructions, which implies to take into account two different structures, the masonry and its backfill, and their interaction. An appropriate tool to model the masonry retaining structure is micro-mechanics computation as finite or discrete element methods.

* Corresponding author; jean-claude.morel@entpe.fr.

Accurate simulations have been performed on either masonry or soil. However, considering the complexity and computational costs of the process, these techniques do not fit yet for practical engineering design.

Therefore, macro-mechanical or even multi-scale simulations have been developed to meet practical expectations.

Concerning masonry mechanical behaviour, modelling developments deal with homogenization. Pande et al. (1989) pioneered this method in order to find equivalent elastic properties. Further developments on homogenization of periodic masonry can be found in Anthoine (1995), Luciano and Sacco (1997) and De Buhan and De Felice (1997); while the first two references resort to limit analysis, the latter is implemented within the field of yield design theory. Significant work has also been performed to provide macroscopic criteria for masonry construction by Lourenço et al. (1998) and Kawa et al. (2008). These studies concentrate on the characterization of the masonry behavior.

Literature on earth pressure analysis is quite abundant, since it is a key issue for most geotechnical engineers. Theoretical earth pressure problems are generally solved using the limit equilibrium method, the slip line method or the upper or lower bound limit analysis. Recent work includes Yang (2007) or Liu and Wang (2008) but these studies only concentrate on the soil, considering the retaining structure as rigid.

This paper presents theoretical and experimental simulations to assess dry joint retaining structures stability. The yield design modelling will first be presented, with special attention paid to the soil/structure interaction. Then, the experimental campaign will be developed, and comparisons with theoretical predictions will be undertaken. As a conclusion, the future perspectives expanding on this work will be exposed.

2 Yield design modelling

The present work relies on yield design (Salençon, 1990); this theory enables to evaluate the ultimate bearing capacity of a structure, solely knowing its geometry, loading mode and yield criterion. This method was first devoted to soil mechanics and it has been later on expanded to masonry (De Buhan and De Felice, 1997; Sab, 2003). The following section relies on both approaches to model a dry joint earth-retaining structure (Fig. 1).

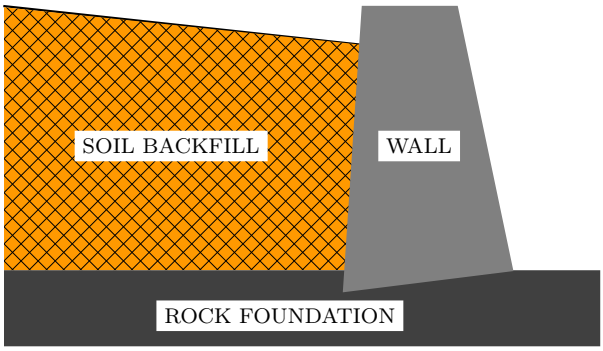

Figure 1. Dry-joint retaining system.

2.1 Hypotheses

The system under investigation is constituted by the masonry retaining structure and its backfill (Fig. 2). The problem will be modelled in the (O, X_1, X_2) plane and for each vector $\underline{V}$ the following notation will be adopted:

$$\underline{V} = V_1 \, \underline{e}_1 + V_2 \, \underline{e}_2$$

Three kinds of parameters of this system are now required to set up yield design.

2.1.1 Geometry

The system considered here (Fig. 2) comprises of a retaining wall of height h, thickness at the top l, batter λ_1, and counter-slope λ_2, and its h_s high backfill, which surface is inclined of β.

2.1.2 Loading process

In this work, it has been considered that there was no boundary loading: therefore, the sole loads acting on the structure are the respective unit weights $\underline{\gamma}_m$ and $\underline{\gamma}_s$ of the masonry and its backfill soil.

2.1.3 Strength criterion

The yield criterion of the system depends on the wall and soil constituent materials. In yield design upper bound approach, the strength criterion of the system is represented by its corresponding support function.

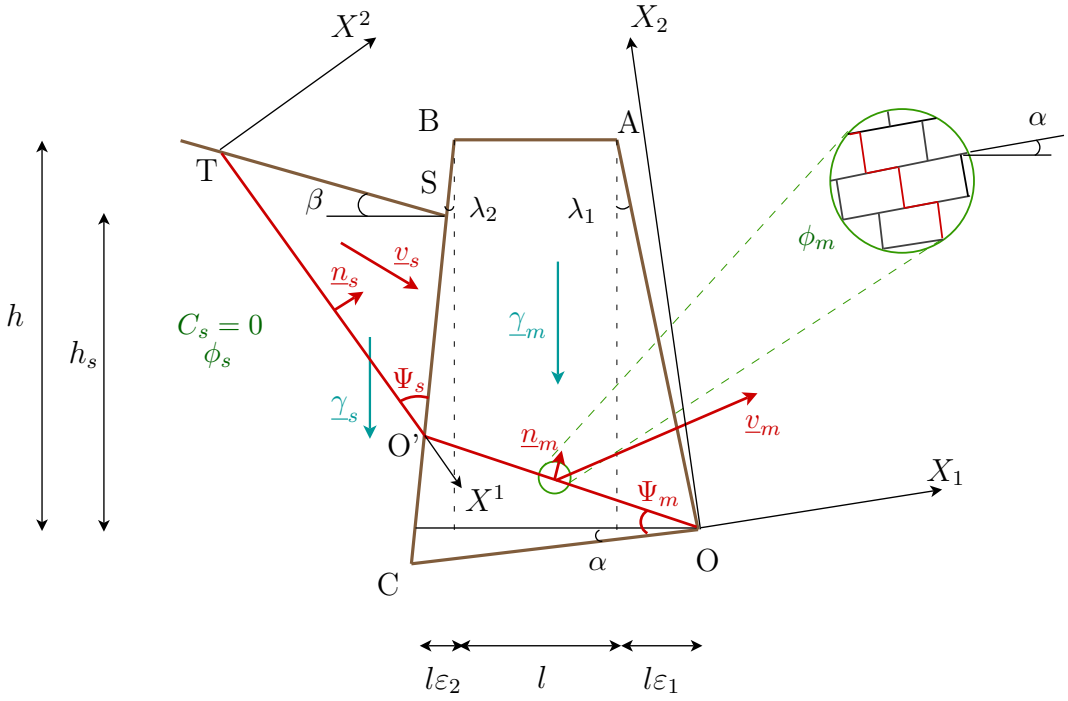

Figure 2. Dry-joint retaining wall modelling: hypotheses of geometry, loading and yield criterion, and failure modes.

2.1.3.1 Masonry strength criterion. The masonry strength criterion is calculated by an homogenization method for periodic media developed on by De Buhan and De Felice (1997). The joints are assumed to have a purely frictional Mohr-Coulomb criterion, only depending on the block friction angle ϕ_m, the stones being considered as infinitely resistant. Thus, the following support function is obtained:

$$\pi\left(\underline{n}_m, [\![\underline{v}_m]\!]\right) = 0 \tag{1a}$$

$$\text{if} \left| \begin{array}{rl} -n_{m1}v_{m1} & \leq 0 \\ \tan\phi_m \left|n_{m1}v_{m1}\right| & \leq m n_{m2}v_{m2} \\ \left|n_{m1}v_{m2} + n_{m2}v_{m1}\right| & \leq -\tan\phi_m\, n_{m1}v_{m1} + \dfrac{1}{\tan\phi_m}\, n_{m2}v_{m2} \end{array} \right. \tag{1b}$$

where m represents the average slenderness ratio of the blocks.

If conditions (1b) are not satisfied, $\pi\left(\underline{n}_m, [\![\underline{v}_m]\!]\right) = \infty$.

2.1.3.2 Soil strength criterion. The soil is considered to be a Mohr-Coulomb material, depending on its cohesion C_s and friction angle ϕ_s. The following support functions (Salençon, 1990) are thus obtained:

$$\pi\left(\underline{d}_s\right) = \frac{C_s}{\tan\phi_s} \mathrm{tr}\left(\underline{d}_s\right) \tag{2a}$$

$$\text{if } \mathrm{tr}\left(\underline{d}_s\right) \leq \left(|d_1| + |d_2|\right) \sin\phi_s \tag{2b}$$

and

$$\pi\left(\underline{n}_s\,,[\![\underline{v}_s]\!]\right) = \frac{C_s}{\tan\phi_s}[\![\underline{v}_s]\!]\,.\,\underline{n}_s \tag{3a}$$

$$\text{if } [\![\underline{v}_s]\!]\,.\,\underline{n}_s \leq |[\![\underline{v}_s]\!]|\,\sin\phi_s \tag{3b}$$

In this study, it has been decided that the cohesion of the soil would not been taken into account ($C_s = 0$) in order to simplify calculations. On the other hand, this hypothesis makes our design calculations better for safety. Consequently, the support functions of the soil vanish to zero. Nevertheless, yield design simulations including soil cohesion can be performed, at the expense of more complex processes.

2.1.3.3 Interface strength criterion. Since there are two entities constituting the system, it is necessary to characterize the interface SC between the back face of the wall and the backfill. It has been decided to model this surface as frictional Coulomb interface (Salençon, 1990) so that:

$$\pi\left(\underline{n}\,,\underline{\Delta v}\right) = 0 \tag{4a}$$

$$\text{if } |\underline{\Delta v}\,.\,\underline{n}| \geq |\underline{\Delta v}\,.\,\underline{t}|\,\tan\delta \tag{4b}$$

where $\underline{\Delta v} = \underline{v}_m - \underline{v}_s$ represents the velocity discontinuity, and δ the friction angle between the soil and the wall.

Considering the toughness of the back face, it has also been decided that the friction angle δ between the wall and the backfill would be taken as:

$$\delta = \min\{\phi_s, \phi_m\} \tag{5}$$

This choice will be discussed later on.

It can be noted that all the support functions involved in this study are equal to zero, meaning that, for all kinematically admissible velocity fields, the maximum resisting work of the system will be null.

2.2 Application of yield design upper bound approach

Yield design upper bound theorem asserts that the structure is stable if the work of the external forces $\mathcal{W}^e$ remain lower than the maximum resisting work $\mathcal{W}^{mr}$ for any kinematically admissible velocity field.

The structure is only submitted to its unit weight (§ 2.1.2); the work of the external forces $\mathcal{W}^e$ can be reduced to:

$$\mathcal{W}^e = \int_{OABO'} \underline{\gamma}_m \cdot \underline{v}_m \, \mathrm{d}V + \int_{STO'} \underline{\gamma}_s \cdot \underline{v}_s \, \mathrm{d}V \tag{6}$$

Considering the strength criteria selected previously, it has been demonstrated that the maximum resisting work vanished to zero:

$$\mathcal{W}^{mr} = 0 \tag{7}$$

under conditions (1b), (2b), (3b) and (4b).

Therefore, the ultimate backfill height the wall can stand verifies:

$$W^e \leq 0 \tag{8}$$

for any kinematically admissible velocity field under conditions (1b), (2b), (3b) and (4b).

In this work, the wall will be intended to break along a failure surface OO' inclined from Ψ_m with normal $\underline{n}_m$. The lower part of the wall $OO'C$ remains fixed whereas the trapezium $OABO'$ is given a virtual velocity $\underline{v}_m$. The soil will fail as a prism along a plane failure surface $O'T$, which forms an angle Ψ_s with the back face of the wall. These two modes of failure are consistent with empirical observations as reported in Constable (1875).

Two different virtual velocity fields of the system will be explored in this study:

- translation of the soil and of the masonry
- shearing of the soil and rotation of the masonry

These velocity fields have been selected because they correspond to classical failure modes in soil (Salençon, 1990) and masonry (De Buhan and De Felice, 1997) mechanics. On the other hand, it will be proved later on that they provide good correspondance as regard to experimental results.

2.3 Ultimate backfill height

2.3.1 Failure by translation of the masonry

In this first simulation, the wall and its backfill will be given translational virtual velocity fields 2.3.1 so that:

$$\begin{aligned} \underline{v}_m &= \underline{\chi}_m = \chi_m \left(\cos\theta_m \, \underline{e}_1 + \sin\theta_m \, \underline{e}_2\right) \\ \underline{v}_s &= \underline{\chi}_s = \chi_s \left(\cos\theta_s \, \underline{e}_1 + \sin\theta_s \, \underline{e}_2\right) \end{aligned} \tag{9}$$

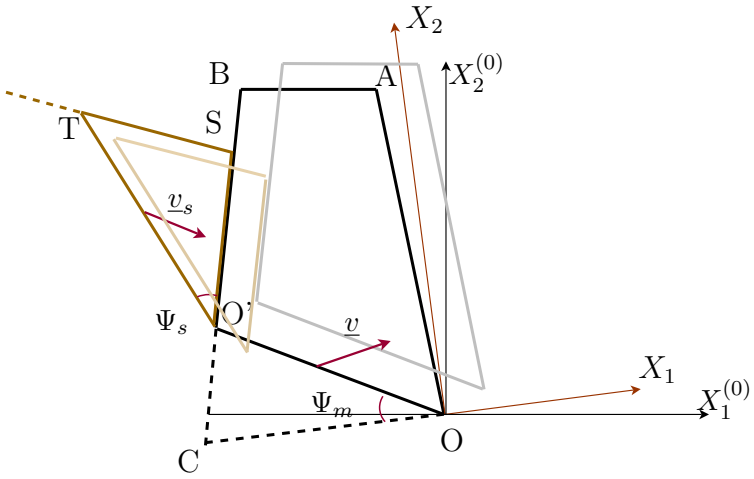

The work of external forces (6) thus can be written as a quadratic polynomial in h_s:

$$W^e = p_2\left(\underline{\chi}_m, \Psi_m, \underline{\chi}_s, \Psi_s\right) {h_s}^2 + p_1\left(\underline{\chi}_m, \Psi_m, \underline{\chi}_s, \Psi_s\right) h_s + p_0\left(\underline{\chi}_m, \Psi_m, \underline{\chi}_s, \Psi_s\right) \tag{10}$$

The maximum resisting work still equals zero but conditions (1b) and (3b) become:

$$\begin{aligned} \chi_m &\leq 0 \\ \tan\phi_m \tan\Psi_m &\leq m \tan\theta_m \\ \tan\phi_m &\leq \tan\theta_m \end{aligned} \tag{11}$$

$$\cos(\theta_s + \Psi_s - \lambda_2) \leq \cos(\frac{\pi}{2} - \phi_s) \tag{12}$$

This interface criterion (4b) causes a relation between χ_m and χ_s:

$$\chi_s \leq \frac{\sin(\theta_\delta - \theta_m)}{\sin(\theta_\delta + \theta_s)} \, \chi_m \tag{13}$$

Considering (8), the system will prove potentially stable for any backfill height h_s ensuring $\mathcal{W}^e$ is negative, which boils down to finding the positive root h_{s0} verifying:

$$\forall\, h_s \in [0, h_{s0}],\ W^e(h_s) \leq 0 \tag{14}$$

The upper-bound value of h_s is given by the minimum of h_{s0} with respect to the kinematic parameters χ_m, θ_m, Ψ_m, χ_s, θ_s, Ψ_s under conditions :

$$h_s^+ = \min_{\chi_m,\theta_m,\Psi_m,\chi_s,\theta_s,\Psi_s} \left\{ h_{s0}(\chi_m, \theta_m, \Psi_m, \chi_s, \theta_s, \Psi_s) \right\} \tag{15}$$

The study of h_{s0} provides $\chi_m^{\text{opt}}, \theta_m^{\text{opt}}, \Psi_m^{\text{opt}}, \chi_s^{\text{opt}}, \theta_s^{\text{opt}}$ and Ψ_s^{opt} so that:

$$h_s^+ = h_{s0}\left(\chi_m^{\text{opt}}, \theta_m^{\text{opt}}, \Psi_m^{\text{opt}}, \chi_s^{\text{opt}}, \theta_s^{\text{opt}}, \Psi_s^{\text{opt}}\right) \tag{16}$$

It can be proved that $\Psi_m^{\text{opt}} = 0$, which means that the optimal sliding surface is the interface between the foundation and the wall. This infers that yield design provides the same numerical result as limit equilibrium analysis for sliding.

2.3.2 Failure by rotation of the masonry

The wall is now given a rotational velocity 2.3.2:

$$\underline{v}_m = -\omega\ \underline{e}_3 \wedge \underline{X} \tag{17}$$

The soil is considered as non-resistant toward traction; it is given a shearing velocity $\underline{v}_s$ 2.3.2 which will be expressed in a referential (T, X^1, X^2) based on the failure line $O'T$:

$$\underline{v}_s = \omega_s \sin\phi_s X^2 \underline{e}^1 + \omega_s \cos\phi_s X^2 \underline{e}^2 \tag{18}$$

The work of external forces (6) is now as a cubic polynomial in h_s:

$$\begin{aligned} \mathcal{W}^e = {} & p_3\left(\omega_m, \Psi_m, \omega_s, \Psi_s\right) {h_s}^3 + p_2\left(\omega_m, \Psi_m, \omega_s, \Psi_s\right) {h_s}^2 \\ & + p_1\left(\omega_m, \Psi_m, \omega_s, \Psi_s\right) h_s + p_0\left(\omega_m, \Psi_m, \omega_s, \Psi_s\right) \end{aligned} \tag{19}$$

Conditions (1b), (3b) and (4b) reduce to:

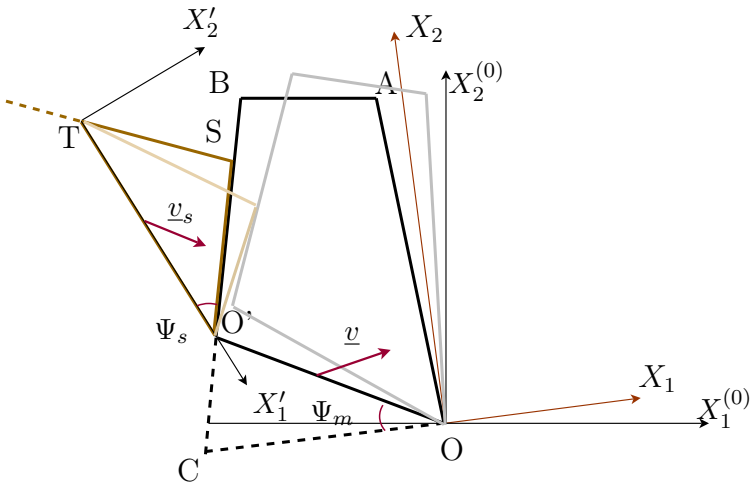

$$\tan \Psi_m \leq \sqrt{\frac{m}{\tan \phi_m}} \tag{20}$$

$$\omega_m \leq \frac{\sin \Psi_m \cos(\Psi_s + \phi_s + \delta)}{\cos \delta} \, \omega_s \tag{21}$$

The masonry can be stable for any backfill height h_s verifying (14); as $\mathcal{W}^e$ is a cubic polynomial in h_s (19), an analytical expression of h_{s0} can be found thanks to Cardano's method. This enables one to calculate the ultimate backfill height h_s^+ as the minimum of h_{s0} with respect to the kinematic parameters ω_m, Ψ_m, ω_s and Ψ_s:

$$h_s^+ = \min_{\omega_m, \Psi_m, \Psi_s} \left\{ h_{s0}(\omega_m, \Psi_m, \omega_s, \Psi_s) \right\} \tag{22}$$

The study of conditions (20) and (21) provides the optimal values of the kinematic parameters so that:

$$h_s^+ = h_{s0} \left(\omega_m^{\text{opt}}, \Psi_m^{\text{opt}}, \omega_s^{\text{opt}}, \Psi_s^{\text{opt}} \right) \tag{23}$$

Numerical simulations show that the optimal failure angle Ψ_m^{opt} is non-null, meaning that for rotational failure, yield design gives a more constraining ultimate backfill height.

Yield design provides an original analytical expression of the ultimate bearing load a dry joint retaining structure can stand, only depending on the strength criterion of the wall and the backfill. In addition, this technique gives an indication on the failure mode of the structure. The relevancy of these results will be evaluated by comparisons with experiments.

3 Parametric analysis : comparison between theoretical and experimental results

The yield design model established previously will be now evaluated by parametrical analysis and confrontation with scale-down experiments. Tests are conducted on 30 cm high masonry structures built with brick and wood blocks, and backfilled till failure with Schneebeli rods. The scale-down models do not respect scaling effects, but they provide a quick and simple evaluation of the dry joint masonry phenomenology.

3.1 Experimental protocol

3.1.1 Constitutive elements characteristics

Two different types of block materials (brick and wood) have been experienced. Each block is about 6 cm long, 2 cm large and 1 cm high. The friction angles of the blocks have been measured thanks to a set of Casagrande tests with a 10x10 cm shear box.

The backfill is made of an analogic soil constituted of small cylinders of duralium called Schneebeli rods, which enables to simulate a 2D soil. These rods are 6 cm long and from 3 to 5 mm in diameter. Their physical characteristics are taken from Hardiyatmo (1995), who measured the friction angle of this analogic soil thanks to a 30x30 cm Casagrande shear box.

All geometrical and physical characteristics used in this study are recorded in Table 1.

3.1.2 Experimental device

The scale-down masonry constructions (Fig. 3) are made of small elements of brick or wood laid dry and based on a rigid foundation of same material as the wall. There are at least five blocks in the wall thickness to validate the use of homogenization. The wall is then backfilled with Schneebeli rods by 1 cm high layers till failure.

3.2 Parametric analysis

The experimental approach aims at assessing the relevancy of the model and its robustness towards a parametric evaluation.

Table 1
Physical and geometrical characteristics of the system (in italic, the parameters which have been tested).

	Brick	Wood
Wall height h (cm)	27.5	
Wall thickness l (cm)	9	11
Wall batter λ_1 (%)	0, *11*, *16*	0, *9*, *12*
Wall counter-slope λ_1 (%)	0	
Joint inclination α (°)	*-12*, *-6*, 0, *6*	*-6*, 0, *6*, *16*
Backfill slope β (°)	0, *10*, *15*, *20*	0, *5*, *10*, *20*
Wall unit weight γ_m (kN/m^3)	18.4	7.1
Backfill unit weight γ_b (kN/m^3)	22.5	
Wall friction angle ϕ_m (°)	33	30
Backfill friction angle ϕ_b (°)	25	

(a) (b)

Figure 3. Experimental device : example of a dry joint wall of wood (a) and test on a brick wall backfilled with Schneebeli rods (b).

Twenty five tests have been performed on different geometrical and physical configurations for the wall or the backfill; the experimental details can be found in Table 1. Three parameters have been tested for each constitutive material: the wall batter λ_1, the joint inclination α, and the backfill slope β. For each range of tests, only one parameter is tested (in italic in Tab. 1), the others being fixed. Each configuration has been tested only once except for the influence of joint inclination on brick walls where two tests have been performed in ordre to assess the repetability of the experimental process.

In Figure 4 can be found theoretical sliding and toppling ultimate capacity as well as the results observed through the experimental process. Theoretical failures are represented in plain lines when they are predominant and in dotted lines when secondary. Experimental heights are figured as triangles, the superposition of two opposite triangles meaning that there were both sliding and toppling failures.

3.2.1 Test on joint inclination

In this first experiment (Fig 4.a), tests were conducted on vertical face walls ($\lambda_1 = \lambda_2 = 0\%$) to investigate the evaluation of the joint inclination influence on dry-joint retaining wall stability. For each type of block, scale-down walls with different configurations for the joint inclination (from $-12°$ to $6°$ for brick, from -6 to $16°$ for wood) have been backfilled ($\beta = 0°$) by layers till failure. Experimental results prove consistent with qualitative theoretical predictions. For example, the brick walls (Fig. 4.1a) slide for $\alpha = -12°$ and topple for α above $0°$. For α between $-9°$ and $-6°$, the wall presents a mixed failure mode, combining sliding and toppling, as predicted by the yield design simulation. Similar results are obtained for wood walls (Fig. 4.2a). For both type of wall, toppling failure angle Ψ_m reaches $45°$, thus validating the theoretical hypothesis of a non-null toppling failure angle, whereas sliding ($\alpha = -12°$ for brick, from $-6°$ to $6°$ for wood) coincides with an observed failure angle of the wall Ψ_m equal to zero, as predicted by yield design. The strong error between experimental and theoretical results on brick walls as $\alpha = -12°$ can be accounted for by the difficulty to build such experimental walls since the strong bed inclination makes the wall very unstable. As for the difference for α between $-9°$ and $-6°$ for brick walls and $\alpha = 6°$ for wood walls, it can be due to the fact that they occur in the transition zone between translation and rotation. Indeed, it can be noticed that several tests have been conducted with the same configuration on brick walls (Fig. 4.1a): they prove the good repetability of the experimental process.

3.2.2 Test on wall batter

The second parametric analysis (Fig 4.b) treats of the influence of wall batter λ_1. Walls have been built with horizontal joints ($\alpha = 0°$) and backfilled with a $20°$ slope. This experiment shows not only good qualitative behaviour but also interesting quantitative predictions: yield design succeeds in estimating the ultimate backfill height a wall can bear with an error rate less than 10%. It has been observed that all sliding failures were located on the foundation ($\Psi_m = 0$).

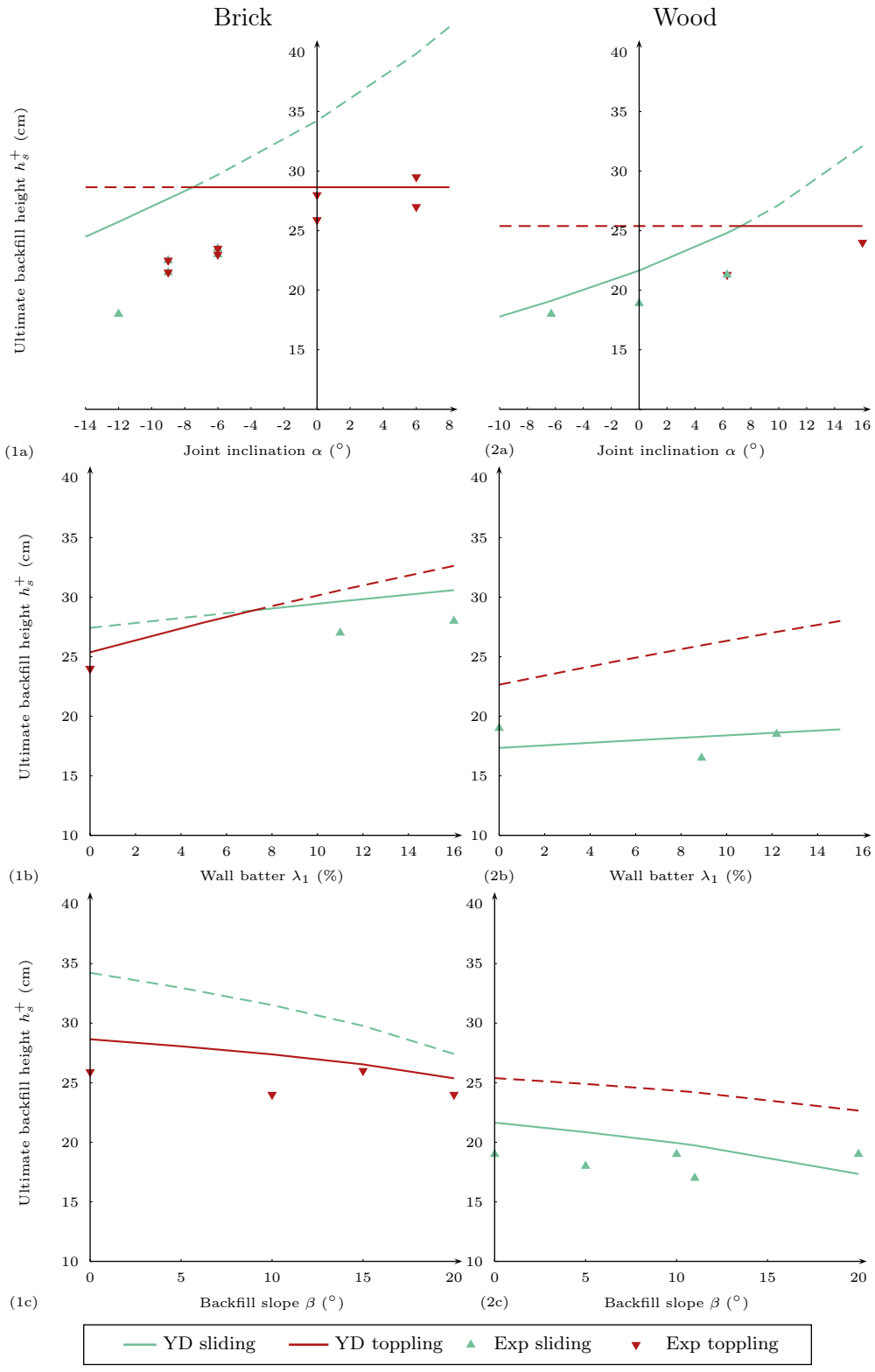

Figure 4. Theoretical and experimental ultimate backfill heights of brick walls ($\gamma_m = 18.4$ kN/m^3, $\phi_m = 33°$) (1) and wood walls ($\gamma_m = 7.1$ kN/m^3, $\phi_m = 30°$) (2) depending on the joint inclination α ($\lambda_1 = 0\%$, $\beta = 0°$) (a), the wall batter λ_1 ($\alpha = 0°$, $\beta = 20°$) (b) and the backfill slope β ($\alpha = 0°$, $\lambda_1 = 0\%$) (c).

3.2.3 Test on backfill slope

This parametric experiment (Fig 4.c) deals with the influence of the backfill slope. Tests have been performed for β varying from its initial value of 0° to 20° on rectangular walls ($\alpha = 0°$ and $\lambda_1 = 0\%$). It confirms the conclusions obtained previously (error rate less than 13%). As for brick walls, the first three models obviously overturned with a failure angle close to 45° whereas the last one ($\beta = 20°$) proves to have a mixed failure mode: it first slightly slides and then topples. All wood walls slid on their foundation.

Experiments prove very good qualitative correspondence with yield design modelling. As for the wall batter and backfill slope parametric tests, there is also close numerical agreement with theoretical predictions. The ultimate backfill height as well as the type of failure estimated by yield design correspond to those found by physical models with an error rate around 10%, thus corroborating the hypothesis adopted for the soil/structure interaction. These results also show that the model is able to take into account different materials and geometry. However, numerical results provided by experiments should be interpreted with caution due to the importance of scale effects.

4 Conclusions

This study has presented a pragmatic method to assess dry joint retaining structures thanks to yield design. 2D scale-down experiments have shown the robustness of this theory towards parametric simulations, thus validating the hypotheses taken in the model. It has been proved that yield design homogenization combined to its upper-bound kinematic approach can be an interesting tool to design or assess dry-joint construction.

Further perspectives on this work concern its application to dry-stone retaining constructions. Dry-stone masonry (interlocking stones fitted without mortar) is a widely expanded form of construction, and an important heritage can be found all around the world. However, no structural design method has been validated until recently. Simulating dry-stone construction by a regular and periodic structure enables to take into account the heterogeneity of the structure while maintaining a pragmatic process. Indeed, this hypothesis can be justified as regard to the apparent regularity (linear bed joints, use of pins to prevent blocks from rotating) of well-built dry-stone masonry (Colas et al., 2008). Full-scale experiments on earth-retaining walls are planned in order to validate the model, with the final objective to set up a criterion, which can be directly exploited for design and assessment of dry-stone walls.

Acknowledgement

The authors would like to acknowledge Julien Bonal and Sébastien Courrier (ENTPE) for their precious collaboration in this experimental campaign.

References

Anthoine, A., 1995. Derivation of the in-plane elastic characteristics of masonry through homogenization. International Journal of Solids and Structures 32 (2), 137–163.

Colas, A., Morel, J., Garnier, D., 2008. Yield design of dry-stone masonry retaining structures – comparisons with analytical, numerical, and experimental data. International Journal for Numerical and Analytical Methods in GeomechanicsUncorrected proof, 16 p.

Constable, C., 1875. Retaining walls – an attempt to reconcile theory with practice. American Society of Civil Engineers 3, 67–75.

De Buhan, P., De Felice, G., 1997. A homogenization approach to the ultimate strength of brick masonry. Journal of the Mechanics and Physics of Solids 45 (7), 1085–1104.

Hardiyatmo, H., 1995. Approche expérimentale du dimensionnement des massifs renforcés à parement cellulaire. Ph.D. thesis, Université Joseph Fourier – Grenoble I.

Kawa, M., Pietruszczak, S., Shieh-Beygi, B., 2008. Limit states for brick masonry based on homogenization approach. International Journal of Solids and Structures 45 (3-4), 998–1016.

Liu, F., Wang, J., 2008. A generalized slip line solution to the active earth pressure on circular retaining walls. Computers and Geotechnics 35 (2), 155–164.

Lourenço, P. B., Rots, J., Blaauwendraad, J., 1998. Continuum model for masonry: parameter estimation and validation. Journal of Structural Engineering 124 (6), 642–652.

Luciano, R., Sacco, E., 1997. Homogenization technique and damage model for old masonry material. International Journal of Solids and Structures 32 (24), 3191–3208.

Pande, G., Liang, J. X., Middleton, J., 1989. Equivalent elastic moduli for brick masonry. Computers and Geotechnics 8, 243–365.

Sab, K., 2003. Yield design of thin periodic plates by a homogenization technique and an application to masonry walls. C. R. Mecanique 331, 641–646.

Salençon, J., 1990. An introduction to the yield design theory and its application to soils mechanics. European Journal of Mechanics A/Solids 9 (5), 477–500.

Yang, X. L., 2007. Upper bound limit analysis of active earth pressure with

different fracture surface and nonlinear yield criterion. Theoretical and Applied Fracture Mechanics 47 (1), 46–56.

List of Figures

List of Tables